Nonsteady-state dissolution of goethite and hematite in response to pH jumps: the role of adsorbed Fe (III)

SHERRY D. SAMSON* AND CARRICK M. EGGLESTON

Department of Geology and Geophysics, University of Wyoming, Laramie, WY 82071 USA

* Author to whom correspondence should be addressed (samson@colorado.edu). Present address: Department of Geological Sciences, University of Colorado, Boulder CO 80309 USA

Abstract—Dissolution transients following downward pH jumps to pH 1 from a variety of higher pH values during dissolution in a mixed-flow reactor contain information about dissolution processes and mechanisms. Despite more than an order of magnitude difference in steady-state dissolution rates, the transients for goethite (α-FeOOH) (this study) and hematite (α-Fe$_2$O$_3$) (Samson and Eggleston, 1998) are similar in their pH dependence and relaxation times. After a pH jump, the time required to reach a new steady state is 40 to 50 hours. The amount of excess Fe released in the transients (defined as the amount of Fe released in excess of that released in an equivalent length of time during steady-state dissolution at pH 1) increases with increasing initial (i.e., pre-jump) pH, and is dependent on initial pH in a manner similar to the pH dependence of Fe^{3+} adsorption to other oxides. We suggest that the excess Fe released in the transients is derived from partial dissolution or depolymerization of the iron (hydr)oxide at pH $\geq$ 1 and the transition of such Fe into the adsorbed state on the mineral surface. Following a pH jump to pH 1, this adsorbed Fe is desorbed by stepwise depolymerization.

1. INTRODUCTION

Mineral weathering has been a subject of geochemical study for at least 150 years because weathering is a key component of elemental cycling at and near Earth's surface, and because there are also a number of industrial and technological reasons for understanding such processes. Among these are mitigating the deleterious effects of scale deposits, through either inhibited growth or engineered dissolution, in settings ranging from production wells to power plants; corrosion control (e.g., iron oxides in particular play an important role in the passivation of metal surfaces); and understanding how pollutants participate in mineral dissolution and growth, and may, through solid solution, become sequestered in secondary products of the weathering of primary minerals.

Great progress has been made in understanding the environmental factors that affect mineral dissolution rates (e.g., pH, saturation state, secondary precipitates, and the presence of organic and other ligands; see Hochella and White, 1990, and White and Brantley, 1995, for reviews). A virtually universal observation made in experimental studies is that dissolution rates often start high and decay toward a steady state. Such transients have been reported for many oxide and silicate minerals: e.g., quartz (Holt and King, 1955), corundum and kaolinite (Carroll-Webb and Walther, 1988), goethite and δ-Al$_2$O$_3$ (Kraemer and Hering, 1997), hematite (Maurice et al., 1995), albite (Holdren and Berner, 1979; Chou and Wollast, 1985;

Hellmann, 1995), biotite (Malmström and Banwart, 1997), diopside (Knauss et al., 1993), and enstatite (Schott et al., 1981). In a few cases, dissolution rates accelerate to a steady state, e.g., quartz at pH > 10 (Knauss and Wolery, 1988).

Transients have often been thought to be limited to the onset of dissolution, and, depending on the solid or the experiment, have been variously attributed to one or more of the following: artifacts of sample preparation, e.g., grinding (Schott et al., 1981; Eggleston et al., 1989), ultra-fine particles (Holdren and Berner, 1979), development of a leached layer (Casey and Bunker, 1990), and nonstoichiometry of the unreacted surface (Burch et al., 1993). Information on rates obtained during the nonsteady-state interval was often discarded as unrepresentative of the reaction of interest, e.g., the long-term dissolution rate of the mineral, and pretreatments such as etching with HF or preconditioning (e.g., 3-4 days of pre-experiment dissolution) have been employed specifically to avoid initial transients (Zinder et al., 1986).

However, observations of recurrent transients in response to cycles in pH (Chou and Wollast, 1984; Spokes and Jickells, 1996), increases in ligand concentration (Mast and Drever, 1987; Wieland and Stumm, 1992; Kraemer and Hering, 1997), and changes in electrolyte composition (Sjöberg, 1989) suggest that in some cases transients contain useful information about dissolution processes. For example, Chou and Wollast (1984) induced recurring dissolution transients for albite by instantaneously

modifying the pH of the input solution in a fluidized-bed reactor, and demonstrated that transients need not be limited to the onset of dissolution. They interpreted the transients as indications of readjustment of altered or leached layers on the feldspar surface in response to the pH jumps. Furthermore, the transition from one steady state to another takes time; the time required for albite to reach a new steady state in response to pH jumps can be 200 hours or more at 25 °C (Chou and Wollast, 1984).

Here, we report the results of pH-jump experiments with goethite (α-FeOOH), compare them to previous results for hematite (Samson and Eggleston, 1998), and use this comparison to explore the role of adsorbed Fe(III) as a reaction intermediate in the dissolution of goethite and hematite. Because the solutions reach a steady state and closely approach equilibrium during the intervals at pH > 1, we show how the idea of adsorbed Fe(III) on hematite surfaces can be fit within a relatively simple surface complexation model.

2. EXPERIMENTAL APPROACH

2.1. Goethite Preparation

Goethite was prepared according to a hydrothermal method using 1 M $Fe(NO_3)_3$ (prepared from $Fe(NO_3)_3 \cdot 9H_2O$; Spectrum reagent A.C.S.) and 5 M KOH (Spectrum reagent, A.C.S.) (Schwertmann and Cornell, 1991). The goethite was suspended in deionized water, centrifuged and decanted several times to remove the finest particles, and aged in deionized water for approximately 30 days. It was again washed and centrifuged twice and dried overnight in a 70°C oven prior to XRD and SEM. Powder XRD (Scintag XDS 2000 Diffractometer equipped with a Cu anode tube) confirmed the goethite structure and SEM (JEOL 35CF) revealed uniform acicular crystals of approximately 1.5 μm in length with no visible amorphous material. The specific surface area, as measured with a Micromeritics TriStar 3000 multipoint N_2 BET surface area analyzer, was 36 $m^2 g^{-1}$.

2.2. Analytical Techniques and Experimental Conditions

Total dissolved Fe effluent concentrations were measured by flame atomic absorption (Perkin Elmer Model 2380 AA spectrophotometer), with a detection limit of 10 ppb Fe. Separate standards were prepared for each experiment from the inlet solutions used in that experiment.

The pH-jump experiments were conducted in a polycarbonate, continuous-flow overhead-stirred tank

reactor (CSTR) at ambient laboratory temperature (22.7 ± 1° C, with the exception of 1 day where the temperature reached 25.8° C) with a Mettler Toledo titration system stirrer motor and stir paddle (input power 4.5V, ~3100 rpm). A discussion of the reactor properties as they relate to mineral dissolution may be found in Samson et al. (2000). CO_2 was not excluded. The reactor was pH-statted (i.e., pH maintained at constant values) using HNO_3 (TraceMetal grade, Fisher Scientific) and NaOH (reagent special grade, A.C.S., Spectrum), with software, burettes, and a voltmeter from McIntosh Analytical Systems. The Ag/AgCl combination electrode (Ross Orion semi-micro model 8305BN) used was calibrated at pH 2.0, 4.0, and 7.0.

A flow rate of 0.6 mL min^{-1} was maintained with variable flow peristaltic pumps. Cell volume was approximately 100 mL, with a goethite concentration of 10 g L^{-1}. Effluent was filtered through a 0.2-μm cellulose acetate membrane (Micro Filtration Systems) mounted in an in-line 47 mm diameter Gelman filter holder at the base of the reactor cell, and collected continuously in acid-washed polypropylene test tubes, 10 minutes per tube for the first two hours following the pH jump and 20 minutes per tube thereafter, with an ISCO 500 Retriever fraction collector.

All solutions were prepared with high-purity, 18.2 MΩ-cm water with total organic carbon ≤ 10 ppb (Milli-Q Plus, Millipore). pH-adjusted input solutions were stored in VWRbrand™ TraceClean amber glass jugs. The pH in the reactor and the input reservoir was changed nearly simultaneously. The pump was attached to a new inlet solution reservoir pre-adjusted to the new pH and the pH change in the reactor was made by pipettor with concentrated acid (16 N HNO_3) or base (8 N NaOH) in order to accomplish the change as quickly as possible (within seconds to minutes) with a minimum increase in volume.

There were two pH-jump experiments in the following sequence of pH: 4.5, 1, 2, 1 for the first experiment and 3, 1 for the second. In each experiment, the first pH jump to pH 1 was preceded by six days of flow at pH 4.5 or pH 3, respectively. Subsequent pH jumps in the first experiment were at 72-hour intervals. The second experiment was unintentionally terminated on the seventh day, six hours after the jump from pH 3 to pH 1.

2.3. Modeling

The kinetic model used to fit our transient data has been justified and described previously (Samson et al., 2000). The overall dissolution rate, $Rate_{diss}$ [mol $m^{-2} s^{-1}$], is the sum of the rates for parallel dissolution reactions (assumed to be first-order) taking place at various types of surface sites. In the model, these var-
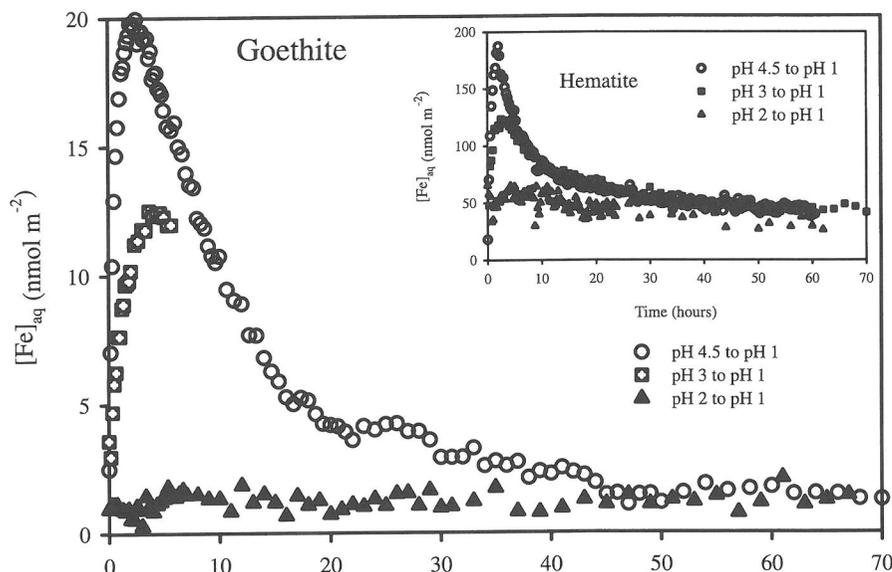
Fig. 1. Results of α-FeOOH pH-jump experiments (this study) with results of α-Fe$_2$O$_3$ pH-jump experiments (Samson and Eggleston, 1998) included for comparison. Each data series represents the Fe outlet concentrations following a pH jump at time 0 from the initial pH indicated to pH 1.

ious surface sites are represented by four groupings of surface sites with similar rate coefficients:

$$Rate_{diss} = k_{SS1}[>Fe_{SS1}] + k_{PI}[>Fe_{PI}] + \\ k_{EXF}[>Fe_{EXF}] + k_{EXS}[>Fe_{EXS}] \quad (1)$$

where $[>Fe_{SS1}]$ [mol m^{-2}] is the constant concentration of Fe surface sites active for dissolution at steady state at pH 1 (> denotes bonds to the surface), $[>Fe_{PI}]$, $[>Fe_{EXF}]$, and $[>Fe_{EXS}]$ [mol m^{-2}] are the concentrations of dissolution-active Fe sites in excess of those present at steady state at pH 1 that are consumed in a pH jump from higher pH to pH 1 (pulse input, fast-dissolving excess, and slow-dissolving excess, respectively), and k_{SS1}, k_{PI}, k_{EXF}, and k_{EXS} [s^{-1}] are the corresponding rate coefficients.

The four groups of sites represent conceptual groupings of surface sites with similar rate coefficients. We are not suggesting that there are only four structural types of surface sites; our macroscopic data provide us with kinetic, not structural, information. The pulse input parameter represents sites whose dissolution is indistinguishable from a pulse input, i.e., the dissolution rate is faster than can be mathematically resolved given the reactor residence time and the sampling interval. The remaining excess dissolution-active sites are consumed at rates which are also indicative of their relative reactivity, one type dissolv-

ing rather quickly ($[>Fe_{EXF}]$) and the other more slowly ($[>Fe_{EXS}]$).

Although we found in previous work (Samson et al., 2000) that at least four groups of surface sites were needed to simultaneously model data from three different solids (α-Fe$_2$O$_3$, α-Al$_2$O$_3$, and In$_2$O$_3$), not all the parameters are needed to describe the data set presented here. Specifically, it was not necessary to use the pulse input parameter, as all rate coefficients were resolvable. We nevertheless include all parameters in the derivation for completeness and applicability to transients other than those presented here.

The total aqueous Fe concentration in the reactor effluent, $[Fe]_{TOT}$ [mol L^{-1}], is the sum of contributions from the four dissolution reactions:

$$[Fe]_{TOT} = \tau A Rate_{SS1}\left(1 - e^{-t/\tau}\right) + A[>Fe_{PI}]e^{-t/\tau} + \\ \tau_{EXF}Ak_{EXF}[>Fe_{EXF}]_o\, e^{-k_{EXF}t}\left(1 - e^{-t/\tau_{EXF}}\right) + \\ \tau_{EXS}Ak_{EXS}[>Fe_{EXS}]_o\, e^{-k_{EXS}t}\left(1 - e^{-t/\tau_{EXS}}\right) \quad (2)$$

where $Rate_{SS1}$ [mol m^{-2} s^{-1}] is the steady-state dissolution rate at pH 1, A [m^2 L^{-1}] is the goethite surface area per unit of solution volume, and τ is a time constant defining the rate of accumulation of Fe within the reactor. Equation 2 is derived from the model (Eqn. 1) and standard chemical engineering ap-

proaches to nonsteady-state processes in mixed-flow reactors (see Samson et al., 2000). For both steady-state dissolution and a pulse input, the time constant equals reactor volume divided by flow rate ($\tau = V\,q^{-1}$), while the time constant for dissolution of the fast- and slow-dissolving excess sites is a function of not only volume and flow rate, but also of the dissolution reaction rate coefficient: $\tau_{EX(F\ or\ S)} = V/(q - Vk_{EX(F\ or\ S)})$.

3. RESULTS AND MODEL FITS

In spite of dissolution rates more than an order of magnitude slower than those of hematite, the goethite dissolution transients following downward pH jumps to pH 1 were remarkably similar to those of hematite in their pH dependence and relaxation times (Fig. 1). We emphasize that the data presented here for both goethite and hematite are for nonsteady-state dissolution *at pH 1*; the periods of time spent at the higher pH conditions serve to allow the surface to generate or regenerate the active sites involved in dissolution at pH 1.

Following the reactor's mixing interval of ~5τ (based on CSTR theory), the reactor outlet concentration directly reflects the dissolution rate. Furthermore, any solute derived from sites whose dissolution is perceived as a pulse input, $[>Fe_{PI}]$, will have been washed out of the reactor, and the outlet concentration attributable to steady-state dissolution at pH 1 will have reached a constant value. Therefore, by subtracting the steady-state outlet concentration from the observed outlet concentrations, the amount of solute derived from the dissolution of $[>Fe_{EXF}]$ and $[>Fe_{EXS}]$ sites can be determined. Assuming the goethite dissolution rate in the interval 5τ to 7.5τ (hours 15 to 22.5) is dominated by dissolution of the slowly dissolving sites, a value for the parameter k_{EXS} can be obtained from the slope of a plot of the natural log of the excess Fe concentration (the measured outlet concentration minus the steady-state concentration) vs. time. The value for k_{EXS} for the

pH jump from pH 4.5 to pH 1 is 0.11 h^{-1}. An independent value for k_{EXS} for the pH 3 to pH 1 transient cannot be determined due to the lack of data in the interval 5τ to 7.5τ. However, previously the hematite results had been successfully modeled with a single value of k_{EXS} for all data sets (see Table 1). Therefore, a value of 0.11 h^{-1} for k_{EXS} was assumed for both goethite transients (pH 4.5 to pH 1, and pH 3 to pH 1), and the remaining model parameters were obtained by nonlinear least-squares fitting of each data set to Eqn. 2.

Figure 2 shows model fits for the transients following pH jumps from pH 4.5 and pH 3 to pH 1 (there was no transient following the pH jump from pH 2) including the relative contributions from two of the three available types of excess dissolution-active sites considered in the model; the use of the pulse input parameter was unnecessary as indicated by zeros in Table 1. The hematite model fits are shown in Fig. 3. Model parameters for the goethite transients are provided in Table 1 along with hematite parameters (Samson et al., 2000) for comparison. Clearly, different amounts of Fe surface sites active for dissolution at pH 1 are generated by aging at different pH values greater than pH 1. Below, we explore how adsorbed Fe might relate to these amounts.

4. DISCUSSION

4.1. Dissolution-active Sites

As in this study of goethite, previous experiments designed to investigate the response of hematite (α-Fe$_2$O$_3$), corundum (α-Al$_2$O$_3$), and cubic In$_2$O$_3$ dissolution rates to abrupt changes in pH (Samson et al., 2000) revealed that following pH jumps to pH 1 from higher pH solutions, a reproducible and regenerable nonsteady-state period of elevated dissolution rate occurs. The results are consistent with the dissolution (at low pH) and rapid regeneration (at higher pH) of a

Table 1. Model parameters (units of Rate$_{SS1}$ are in terms of moles of Fe) with hematite parameters (Samson et al., 2000) for comparison. A value of zero indicates use of the parameter was not required in order to fit the data.

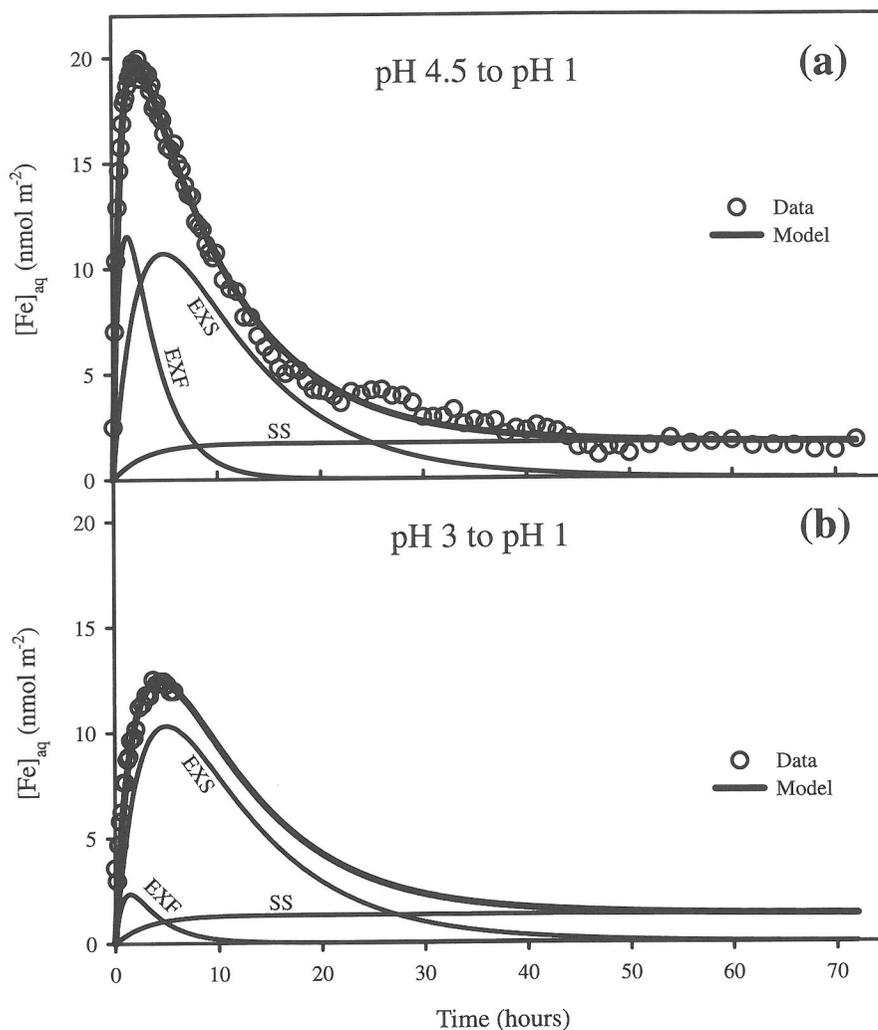| Mineral	α-FeOOH	α-FeOOH	α-Fe$_2$O$_3$	α-Fe$_2$O$_3$	α-Fe$_2$O$_3$	α-Fe$_2$O$_3$	α-Fe$_2$O$_3$
Initial pH	3	4.5	2	2.5	3	4.5	6
k_{EXF} [h^{-1}]	1.29	1.29	0	0.78	0.78	0.78	0.78
k_{EXS} [h^{-1}]	0.11	0.11	0.07	0.07	0.07	0.07	0.07
$[>Fe_{PI}]_o$ [nmol m^{-2}]	0	0	43	0	0	0	0
$[>Fe_{EXF}]_o$ [nmol m^{-2}]	4	19	0	100	96	249	316
$[>Fe_{EXS}]_o$ [nmol m^{-2}]	51	57	217	363	717	772	804
Rate$_{SS1}$ [pmol m^{-2} s^{-1}]	0.17	0.17	5.6	7.2	7.8	8.6	6.9
Total Excess [nmol m^{-2}]	55	76	260	463	813	1021	1120

Fig. 2. Model fits for α-FeOOH transients following pH jumps to pH 1 from (a) pH 4.5 and (b) pH 3. EXF, EXS, and SS represent contributions to the total modeled dissolution from fast- and slow-dissolving excess sites and steady-state dissolution, respectively.

form of dissolution-labile metal ion at the oxide surface. We equate such dissolution-labile sites with active sites for dissolution.

Surface complexation models for steady-state dissolution assume a constant ratio of active sites to total (active and less active) sites, with the understanding that dissolution is favored at a relatively small fraction of active sites with relatively low activation energies (Furrer and Stumm, 1986; Wieland et al., 1988). A departure from a steady-state rate of dissolution in response to a change in conditions implies a corresponding change (i.e., increase or decrease) in the concentration of dissolution-active sites. Where do

such sites originate? A number of possibilities have been suggested, including the formation of altered or leached layers on the feldspar surface (Chou and Wollast, 1984), aspects of surface topography such as surface roughness and crystal defects (Helgeson et al., 1984; Lasaga and Blum, 1986), and the presence of secondary phases.

Another possibility is the presence of adsorbed "nutrient," e.g., Fe^{3+} on hematite, as postulated by Burton-Cabrera-Frank (BCF)-type theories of crystal growth and dissolution (Burton et al., 1951). Here, the term "adsorbed" refers to surface Fe^{3+} that has no more than three bonds to the surface (i.e., no greater
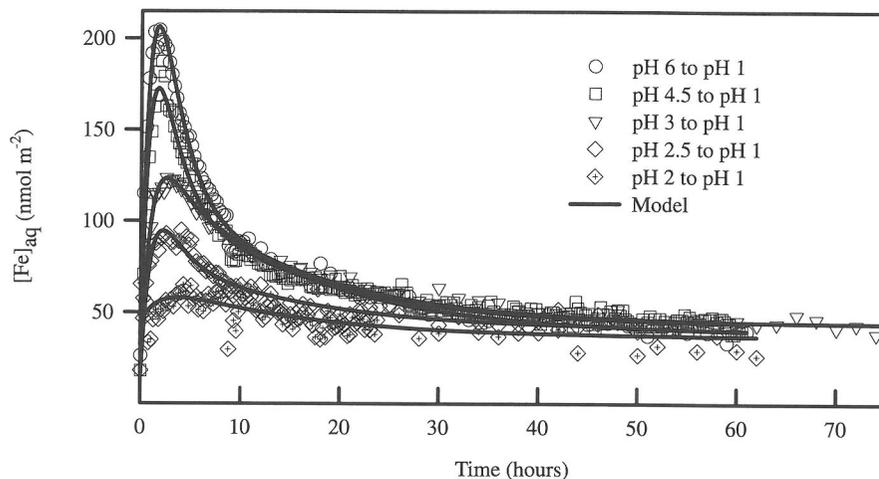
Fig. 3. Model fits for α-Fe_2O_3 transients following pH jumps to pH 1 at time 0 from the initial pH indicated.

polymerization than Fe^{3+} at kink sites) and that may occupy surface sites that are distinct from the terminated bulk hematite structure. Although by definition this includes Fe^{3+} that may be adsorbed or precipitated from solution during an upward jump in pH, we must emphasize that this source of Fe alone cannot account for the amount of Fe that is released in the transients following subsequent downward pH jumps (Samson and Eggleston, 2000; Samson et al., 2000). Iron released in the transients must also include Fe extracted from the terminated bulk hematite structure by depolymerization into the more labile adsorbed state (e.g., surface complexes such as kink sites, ledges, and adatoms). To support these ideas, and to introduce the basic issues involved, we briefly review earlier investigations that attributed dissolution transients to adsorbed "nutrient".

4.2. Lattice Metal Ions as Adsorbates

Holt and King (1955) noted that quartz and amorphous silica dissolve with an initial rapid dissolution transient. Artifactual disturbed layers due to grinding and other theories for the high-rate transient were proposed. However, surface electron diffraction showed no disordered surface layer (Holt and King, 1955). They dissolved a "disturbed" layer on a pretreated quartz powder in alkaline (pH ~13) solution and found that immersion of the resulting powder in an *undersaturated* silica solution at pH 8 produced a gradual *decrease* in the silica concentration over a period of 16 to 20 hours, which they attributed to silica adsorption. Redissolution of this powder at pH 13

gave another initial transient. Therefore, the initial transient was restored by adsorption of silicic acid. They also found, using ^{31}Si, that the original powder would exchange with silica in solution, i.e., the ^{31}Si was diluted by adsorption-exchange with the surface, suggesting that an adsorbed-silica layer forms.

Bergman and Patterson (1961) also found that silica would adsorb to etched quartz surfaces. The model for dissolution and precipitation of amorphous silica by Fleming (1986) explicitly includes adsorption of silicic acid, and Thornton and Radke (1988) also invoked a silica adsorption step in their kinetic model for silica dissolution and condensation. Gratz and Bird (1993) gave a detailed steady-state model for quartz dissolution based on BCF theory (Burton et al., 1951) and consideration of different types of adsorbed silica groups at the quartz surface.

These observations imply that lattice ions of oxides can adsorb to the oxide surface; further, they can be potential-determining ions. The idea that Fe(III) can be a potential-determining ion on Fe(III) oxides, for example, is not new. This possibility was one reason for Parks' (1965) examination of the relationship between the pH of point of zero charge for Fe(III) oxide minerals and the isoelectric points, or equivalence points, of aqueous Fe(III) species. Parks and de Bruyn (1962) and Parks (1965) suggested that one way to view surface charge on hematite is to consider slight dissolution of hematite, followed by readsorption of hydrolyzed Fe ions. Fuerstenau (1970) pointed out that surface charge on oxides could be accounted for by "Adsorption-dissociation of H^+ from surface hydroxyls...[or] partial dissolution of the oxide and
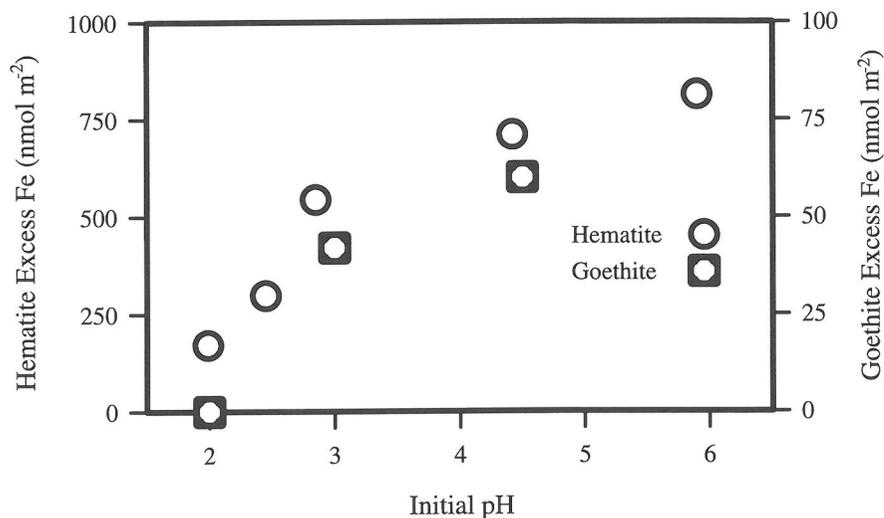
Fig. 4. The amount of excess Fe released in 15 h following downward pH jumps to pH 1, from the initial pH indicated, for goethite (this study) and hematite (Samson and Eggleston, 1998). The amount of excess Fe released following the goethite pH jump from pH 3 is an estimate based on the available 6 hours of data and the model projections (see Fig. 2). Analytical error is within the size of the data points; the determination of excess Fe, however, is also sensitive to the choice of steady state.

formation of hydroxyl complexes in solution, followed by adsorption of these complexes." These earlier ideas have not been greatly explored in the past two decades, but the nonsteady-state dissolution observations have forced us to re-examine them.

4.3. Adsorption of Fe(III) on Hematite

A Mössbauer study of Fe^{3+} adsorption on hematite (Ambe and Ambe, 1990) reported 60% adsorption of Fe^{3+} at pH 2.5. Furthermore, adsorption of Fe(III) on several other solids, including α-SiO_2 and α-Al_2O_3, has been studied (Parks, 1990), and the adsorption edge (i.e., the pH at which 50% of the total amount of a solute cation is adsorbed) is between pH 2 and pH 4, independent of the solid. This is consistent with the general observation that metal ions adsorb roughly at the pH where they start to hydrolyze (James and Healy, 1972; Hachiya et al., 1984a;b); the onset of hydrolysis appears to be more important than the properties of the surface (Fuerstenau, 1970).

Consistent with the latter observation, despite the differences between goethite and hematite crystal structure, dissolution rate, and the amounts of Fe released in the transients following downward pH jumps, the transients exhibit the same pH dependence (Fig. 4). Moreover, the amount of excess Fe released in the transients for both minerals is pH-dependent in a way similar to the pH dependence of Fe^{3+} adsorption to other oxides (Fig. 4). A similar relation to the pH dependence of adsorption was observed for the release of excess Al in pH jump experiments with corundum (Samson et al., 2000).

Here we consider, within the context of existing surface complexation ideas, the formation of adsorbed Fe(III) on iron oxide, and its subsequent dissolution. Because (1) the solubilities of hematite and goethite are extremely low at pH > 3, (2) pH jumps back to pH > 1 from pH 1 involve transient supersaturation, (3) it is extremely difficult to make solutions with less than ppb Fe impurities, and (4) we have observed very little difference in the dissolution transients from non-flowing versus flowing reactors at pH > 3, we assume that equilibrium is closely approached during the times spent at pH > 1 in order to show how adsorbed Fe(III) can be understood within an equilibrium surface complexation model.

Consider an aqueous solution in equilibrium with hematite at pH 1. The predominant aqueous species of Fe(III) in equilibrium with hematite under these conditions is Fe^{3+}(aq). Small amounts of strong base are added to adjust the pH upward and, as pH rises, the amount of Fe^{3+} that can exist in solution in equilibrium with hematite falls at a rate of 3 orders of magnitude per pH unit. Thus, raising the pH from 1 to 2 will cause Fe(III) to attach to the hematite surface. This at-

Table 2. Reactions (> denotes a surface site) and equilibrium constants used for fitting in MICROQL (diffuse double layer model, capacitance 1 F m-2, site density 9.4 g L-1, surface area 4.8 m2 g-1, ionic strength 0.1).

Reaction	Log K	Ref.
$0.5\alpha\text{-}Fe_2O_3 + 3H^+ = Fe^{3+} + 1.5H_2O$	−2.057	(a)
$0.5\alpha\text{-}Fe_2O_3 + 2H^+ = FeOH^{2+} + 0.5H_2O$	−4.247	(b)
$0.5\alpha\text{-}Fe_2O_3 + H^+ + 0.5H_2O = Fe(OH)^{2+}$	−7.727	(b)
$0.5\alpha\text{-}Fe_2O_3 + 1.5H_2O = Fe(OH)_3^0$	−15.79	(c)
$0.5\alpha\text{-}Fe_2O_3 + 2.5H_2O = Fe(OH)_4^- + H^+$	-23.657	(b)
$>FeOH = >FeO^- + H+$	-11.3	(d)
$>FeOH + H^+ = >FeOH_2^+$	5.7	(d)
$0.5\alpha\text{-}Fe_2O_3 + >FeOH + H^+ + H_2O = (>FeO)FeOH^+ + 1.5H_2O$	3.4	(e)
$0.5\alpha\text{-}Fe_2O_3 + >FeOH + 2H^+ = (>FeO)Fe^{2+} + 1.5H_2O$	7.5	(e)
$0.5\alpha\text{-}Fe_2O_3 + 2>FeOH = (>FeO)_2FeOH^0 + 0.5H_2O$	2.67	(e)
$0.5\alpha\text{-}Fe_2O_3 + 3>FeOH + H^+ = (>FeO)_3FeH^+ + 1.5H_2O$	12.9	(e)
$0.5\alpha\text{-}Fe_2O_3 + 3>FeOH = (>FeO)_3Fe^0 + 1.5H_2O$	6.8	(e)

(a) Calculated from the Gibbs free energy value for hematite from Hemingway
(1990) and free energy values for Fe^{3+} and H_2O from Wagman et al. (1982).

(b) Calculated using hydrolysis constants from Baes and Mesmer (1976).

(c) Calculated using the hydrolysis constant from the MINTEQA2 database (Allison
et al., 1991).

(d) Sahai and Sverjensky (1997).

(e) Obtained by trial-and-error fitting (this study).

tachment must in all likelihood proceed by the stepwise attachment of single bonds. Adopting a traditional 2-pK model for surface sites (i.e., the surface is assumed to consist of $>FeOH_2^+$, $>FeOH$ and $>FeO^-$ sites), the first adsorbed Fe complex to form might be written stoichiometrically as:

$$> FeOH + Fe^{3+} = (> FeO)Fe^{2+} + H^+ \quad (3)$$
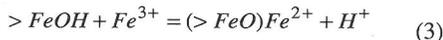
This adsorption process forms a positively charged surface complex despite releasing a proton. Of course, $>FeOH$ sites are scarce at low pH, but the adsorption of a trivalent cation to other, positively charged surface sites is much more energetically unfavorable. After the formation of one bond to the solid, more bonds to the surface can form:
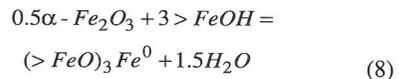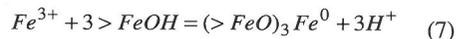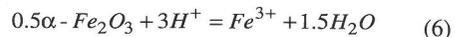
$$(> FeO)Fe^{2+} + > FeOH = (> FeO)_2 Fe^+ + H^+ \quad (4)$$
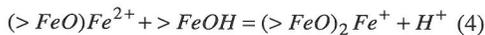
that repolymerize the adsorbed Fe(III) to the solid. Taken one step further, we can form a neutral surface Fe(III) site according to:

$$(> FeO)_2 Fe^+ + > FeOH = (> FeO)_3 Fe^0 + H^+ \quad (5)$$
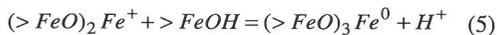
Equations 3-5 release three protons as part of polymerizing aqueous Fe^{3+} onto a hypothetical hematite surface. If we add Eqn. 6 for the dissolution of hematite (in order to create aqueous Fe^{3+}) to the sum of reactions 3-5 (Eqn. 7), the resulting equation (Eqn. 8) describes the formation of neutral adsorbed-Fe sur-

face sites via the consumption of hematite (we emphasize that all equations here are equilibrium, not kinetic, expressions):

$$0.5\alpha\text{-}Fe_2O_3 + 3H^+ = Fe^{3+} + 1.5H_2O \quad (6)$$

$$Fe^{3+} + 3 > FeOH = (> FeO)_3 Fe^0 + 3H^+ \quad (7)$$

$$0.5\alpha\text{-}Fe_2O_3 + 3 > FeOH =$$
$$(> FeO)_3 Fe^0 + 1.5H_2O \quad (8)$$

This reaction does not involve H^+ directly, although the number of available $>FeOH$ sites is pH-dependent. Equations 3-8 provide an equilibrium framework for the adsorption of Fe(III) to hematite surfaces that is consistent with the overall stoichiometry of hematite dissolution and with solubility equilibrium between hematite and solution. In essence, they allow for a form of Fe that is neither hematite bulk solid nor aqueous solute. It should be remembered that prior to pH jumps from higher pH conditions to pH 1, after which dissolution output is monitored, the samples have been aged in the higher pH solutions for periods of up to a week. Experiments in which the samples were aged at the higher initial pH for various amounts of time show that the dissolution transients can be regenerated in a very short time, after which aging time does not have much effect on the amount of iron involved in a subsequent transient induced by a jump to pH 1 (Samson and Eggleston, 2000). As we have

stated above, there is thus a very defensible basis for assuming that equilibrium was closely approached during aging at the initial pH conditions, and thus the use of equilibrium adsorption modeling to better understand the role of adsorbed Fe in the dissolution transients is reasonable.

In addition to the reactions above that depict changes in the polymerization of surface or adsorbed Fe(III) on hematite, there are protonation-deprotonation reactions that change the charge of adsorbed-Fe(III) sites in a manner analogous to hydrolysis of aqueous species in solution, e.g.:
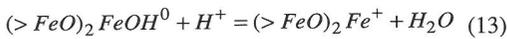
$$(> FeO)_2 Fe^+ + H_2O = (> FeO)_2 FeOH^0 + H^+ \quad (9)$$

and

$$(> FeO)Fe^{2+} + H_2O = (> FeO)FeOH^+ + H^+ \quad (10)$$
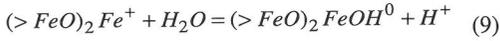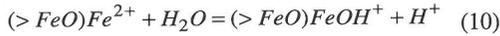
The product of Eqn. 9 (resulting from hydrolysis on the surface) is the same as the product of Eqn. 11 below (adsorption of hydrolyzed species):

$$2 > FeOH + FeOH^{2+} = (> FeO)_2 FeOH^0 + 2H^+ \quad (11)$$
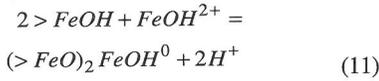
By simply reversing the sequence of polymerization above (i.e., by adding a proton) we can force surface Fe closer to the dissolved state, e.g.:

$$(> FeO)_2 FeOH^0 + H^+ = > FeOH + (> FeO)FeOH^+ \quad (12)$$
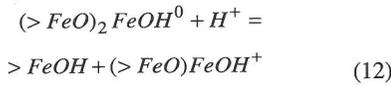
or we may create charged surface sites, e.g.:

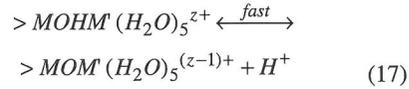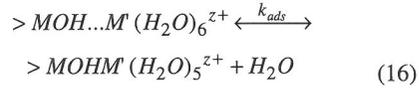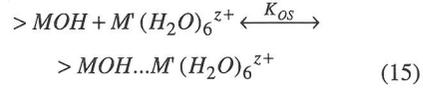$$(> FeO)_2 FeOH^0 + H^+ = (> FeO)_2 Fe^+ + H_2O \quad (13)$$

Thus protonation can have different effects depending upon whether a bridging oxygen or terminal hydroxyl is protonated, and these differences are very likely to have significant kinetic consequences. Finally, and in analogy to the structure of goethite, adsorbed Fe may be bonded to the surface via one or more bridging hydroxyls according to:

$$(> FeO)_2 Fe^+ + (> FeOH) = (> FeO)_2 (> FeOH)Fe^+ \quad (14)$$
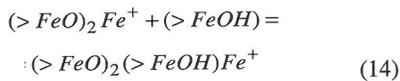
The surface species $(>FeO)_2(>FeOH)Fe^+$ formed in Eqn. 14 is indistinguishable from that formed in the forward progress of Eqn. 13 on the basis of any aqueous species, but the presence or absence of a bridging hydroxyl can have important kinetic implications. Therefore we include such species in the surface complexation modeling below.

Hachiya et al. (1984a,b) have shown that the kinetics of metal ion adsorption to alumina are best described by the following sequence of reactions:

$$> MOH + M'(H_2O)_6^{z+} \xleftarrow{K_{OS}} > MOH...M'(H_2O)_6^{z+} \quad (15)$$

$$> MOH...M'(H_2O)_6^{z+} \xleftarrow{k_{ads}} > MOHM'(H_2O)_5^{z+} + H_2O \quad (16)$$

$$> MOHM'(H_2O)_5^{z+} \xleftarrow{fast} > MOM'(H_2O)_5^{(z-1)+} + H^+ \quad (17)$$

where M is the metal ion of the solid and M' is the sorbing metal ion. The formation of an outer-sphere complex (denoted by OS in Eqn. 15) is followed by the loss of a water molecule from the inner sphere of the adsorbing metal ion (in general, even if a metal is hydrolyzed, water loss from the inner hydration sphere is faster than hydroxyl loss; Margerum et al., 1978). This leads to the formation of an inner-sphere hydroxyl-bridged complex that may in turn deprotonate to form an oxygen-bridged inner-sphere complex. Apparently bridging OH^- is an important intermediate in the overall adsorption-desorption process and there is no *a priori* reason that the same process should not also apply to iron oxides.

One way to view active sites in the nonsteady-state dissolution of hematite, then, is as adsorbed Fe that desorbs at pH 1 in response to a downward pH jump from a higher initial pH. The source of such adsorbed Fe would be reactions in which Fe(III) adsorbs to hematite surface sites at slightly acidic to neutral pH (whether by adsorption from solution or by depolymerization of the solid, i.e., Eqn. 8). By aging the hematite and goethite suspensions at various pH values before a pH jump, we may have approached equilibrium with respect to a surface configuration of Fe(III) sites of the types proposed in Eqns. 3-5, 9, and 10. The rapidity with which dissolution-active sites on hematite are regenerated upon return to higher pH from pH 1 (within minutes or less; Samson and Eggleston, 2000) suggests that the intervals at higher pH in these studies (from 3 to 6 days) should be more than adequate for the distribution of surface sites to equilibrate. Therefore, we can inquire experimentally whether the amount of Fe released in a nonsteady-state transient bears any relation to calculated amounts of adsorbed Fe.

Figure 5 shows the result of trial-and-error fitting of calculated abundances of various Fe surface sites to the amount of Fe released after a pH jump that, by our model, corresponds to pulse input (*PI*), fast-dis-
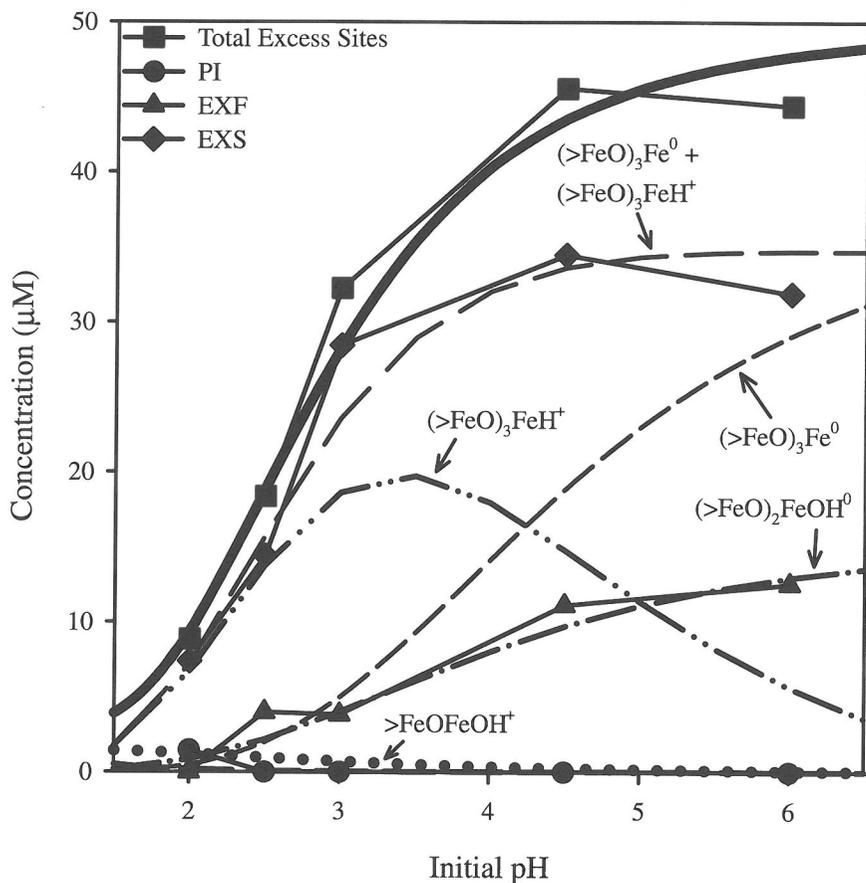
Fig. 5. MICROQL (Westall, 1979) calculations of hypothetical adsorbed Fe surface sites on hematite, as a function of initial pH, and fitted model parameters from hematite pH-jump experiments (Samson and Eggleston, 1998): pulse input (PI), fast-dissolving (EXF) and slow-dissolving (EXS) excess sites, and total excess sites. The heavy solid line represents the calculated total of the Fe surface sites illustrated. Reactions, equilibrium constants, and model assumptions are provided in Table 2.

solving (*EXF*), and slow-dissolving (*EXS*) excess sites (using MICROQL; Westall, 1979). Note that the data points in Fig. 5 are the initial surface concentrations of the different types of excess surface sites derived from our experimental data; another way to view this is that the integrated amount of Fe released in each dissolution transient represents an amount of what we have described as adsorbed Fe created by virtue of the time spent at the initial, higher pH. There is a correspondence between the behavior of *PI* sites and the calculated $>FeOFeOH^+$ sites, between *EXF* sites and the calculated $(>FeO)_2FeOH^0$ sites, and between *EXS* sites and the calculated sum of the triply-bonded sites $(>FeO)_3Fe^0$ and $(>FeO)_3FeH^+$. The latter site represents Fe adsorbed to two $>FeO^-$ sites and one $>FeOH$ site, i.e., $(>FeO)_2(>FeOH)Fe^+$ with one bridging hydroxyl. The rate coefficients for

the surface sites proposed in the model correspond with the degree of polymerization of the hypothetical adsorbed-Fe surface sites: the greater the degree of polymerization, the smaller the rate coefficient (i.e., the slower the dissolution).

Use of a greater variety of surface sites did not improve the fit substantially. In addition, fitting of the slow-dissolving excess sites (*EXS*) with less-polymerized species was much less satisfactory. While it is clearly hazardous to make too much of the structural nature of stoichiometric combinations of Fe, surface sites and protons, we did find that any stoichiometric combination involving only two surface sites (i.e., doubly polymerized to the surface) could not adequately fit the concentration versus pH dependence of the total or *EXS* sites active for dissolution at pH 1.

4.4. Effect of Structural OH⁻ in Goethite on Surface Ligand Exchange

The idea that surface Fe sites attached to the solid via bridging OH^- may be subject to particularly slow dissolution rates is intriguing. First, goethite, with structural OH^-, dissolves more slowly at steady state on a total-surface-area-normalized basis than does hematite. In fact, in mixtures of goethite and hematite, all the hematite dissolves before the goethite, even when the hematite is in excess (Cornell and Giovanoli, 1993). Goethite also dissolves more slowly than does hematite during nonsteady-state dissolution transients on a per site basis. However, rate constants for nonsteady-state dissolution vary by less than a factor of two between hematite and goethite. The major difference appears to lie simply in the lower number of dissolution-active sites for goethite.

Dissolution of hematite does not appear to take place preferentially at specific crystal faces. Cornell and Giovanoli (1993), using seven different samples of hematite prepared by different methods and with different morphologies, found a linear relationship between rates of acid dissolution and surface area, independent of surface morphology. However, it has been shown that dissolution of acicular synthetic goethite crystals similar to those used in this study is anisotropic and takes place preferentially on the (001) and (010) faces compared to the (100) face (Cornell et al., 1974). Thus, one explanation for the smaller number of active sites on goethite is simply that less of the surface is participating in active dissolution. This, however, requires an explanation of why some goethite surfaces are apparently inactive. Cornell et al. (1974) point out that the (001) face contains only singly coordinated hydroxyls (i.e., coordinated to one iron atom). The (010) face contains singly and doubly coordinated hydroxyls, whereas the (100) face includes hydroxyls coordinated to 1, 2, and 3 Fe atoms. This suggests the possibility that dissolution-active sites are associated with the singly coordinated hydroxyls, and that slow dissolution is associated with bridging hydroxyls. Whether or not this is due to effects upon local ligand exchange rates is unknown.

We cannot measure directly the ligand exchange rates of surface metal centers, and the coordinative possibilities are more numerous and complex than for aqueous ions. Nevertheless, the reactivity trends of aqueous ions can provide clues to trends in oxide mineral dissolution kinetics. For example, the steady-state proton-promoted dissolution rates of some simple oxides, nesosilicates, and trivalent sesquioxides correlate with the rates of water exchange at the corresponding aqueous ions (Casey, 1991; Casey and Westrich, 1992; Samson et al., 2000). Westrich et al. (1993) also found that the dissolution rates at pH 2 of mixed-cation nesosilicates scale in the same manner as the stoichiometrically-weighted average water exchange rates of the corresponding aqueous cations. Since mineral dissolution is fundamentally a process of ligand exchange, the inference is that the rates of surface ligand exchange for these minerals trend with the rates of water exchange for the aqueous ions.

Hydrolysis, in general, has a labilizing effect on the rates of water exchange at aqueous cations (Margerum et al., 1978), resulting in a trend of increasing rates of water exchange with increasing solution pH, and observations from previous studies (Samson and Eggleston, 1998; Samson et al., 2000) suggest that hydroxylation of the mineral surface with increasing pH has a similar labilizing effect on the rates of ligand exchange of surface metal centers. Consistent with this idea, a study exploring the kinetics of the regeneration of dissolution-active sites on hematite at pH 3 and pH 6 (Samson and Eggleston, 2000) demonstrated that dissolution-active sites are regenerated within minutes or less upon a return to higher pH from pH 1. This labilization, however, may not lead to dissolution unless there is a sufficient supply of protons to aid net depolymerization rather than merely the rapid exchange of surface Fe sites between different polymerized configurations. Protonation, therefore, can have opposing effects. It can participate in the depolymerization of structural or adsorbed Fe, facilitating dissolution, but it may also decrease the ligand exchange rate of the surface metal center, inhibiting dissolution. Here, the response of hematite and goethite dissolution rates to pH jumps allows us to compare, to a first approximation, a case in which the surface ligands that coordinate adsorbed Fe(III) surface sites are likely to be protonated (i.e., bridging hydroxyl in goethite) with a case in which they likely are not (bridging oxygen in hematite). We speculate that the slower dissolution rates for goethite as compared to hematite, under both steady- and nonsteady-state conditions, may be due to inhibition of surface ligand exchange rates by structural OH^- in goethite.

5. SUMMARY AND CONCLUSIONS

Although the dissolution rates of goethite are more than an order of magnitude less than those of hematite, under both steady- and nonsteady-state conditions, the relaxation times of dissolution transients following downward pH jumps to pH 1 from various higher pH values are nearly identical. Furthermore, the amount of excess Fe released in the transients for both minerals is pH-dependent in a way similar to the pH dependence of Fe^{3+} adsorption to other oxides.

We suggest that the excess Fe released in the transients is derived from partial dissolution or depolymerization of the iron (hydr)oxide at pH ≥ 1 followed by readsorption of Fe to the mineral surface. Following a pH jump to pH 1, this adsorbed Fe is desorbed by stepwise depolymerization. The slower dissolution rates of goethite relative to hematite appear to be related to bridging hydroxyl; our speciation of adsorbed Fe on hematite also associates slowly dissolving sites with bridging OH⁻. The exact reason for this association is not clear, but is likely related to effects upon local acidity constants, ligand exchange rate, and rates of back-reaction.

REFERENCES

Allison J. D., Brown D. S., and Novo-Gradac K. J. (1991) MINTEQA2/PRODEFA2, A geochemical assessment model for environmental systems. U.S. Environmental Protection Agency.

Ambe S. and Ambe F. (1990) Mössbauer study of ferric ions adsorbed at α-ferric oxide/aqueous solution interface. *Langmuir* **6**, 644-649.

Baes C. F. Jr. and Mesmer R. E. (1976) *The Hydrolysis of Cations*. John Wiley & Sons, Inc., New York.

Bergman I. and Paterson M. S. (1961) Silica powders of respirable size. I. Preliminary studies of dissolution rates in dilute sodium hydroxide. *J. Appl. Chem.* **11**, 369-376.

Burch T. E., Nagy K. L., and Lasaga A. C. (1993) Free energy dependence of albite dissolution kinetics at 80 °C and pH 8.8. *Chem. Geol.* **105**, 137-162.

Burton W. K., Cabrera N., and Frank F. C. (1951) The growth of crystals and the equilibrium structure of their surfaces. *Phil. Trans. Roy. Soc. London Ser. A.* **243** (A.866), 299-358.

Carroll-Webb S. A. and Walther J. V. (1988) A surface complex reaction model for the pH-dependence of corundum and kaolinite dissolution rates. *Geochim. Cosmochim. Acta* **52**, 2609-2623.

Casey W. H. (1991) On the relative dissolution rates of some oxide and orthosilicate minerals. *J. Colloid Interface Sci.* **146**, 586-589.

Casey W. H. and Bunker B. (1990) Leaching of mineral and glass surfaces during dissolution. In *Mineral-Water Interface Geochemistry* (eds. M. F. Hochella Jr. and A. F. White). Reviews in Mineralogy Vol. 23, Mineralogical Society of America, Washington, D.C. pp. 397-426.

Casey W. H. and Westrich H. R. (1992) Control of dissolution rates of orthosilicate minerals by divalent metal-oxygen bonds. *Nature* **355**, 157-159.

Chou L. and Wollast R. (1984) Study of the weathering of albite at room temperature and pressure with a fluidized bed reactor. *Geochim. Cosmochim. Acta* **48**, 2205-2217.

Chou L. and Wollast R. (1985) Steady-state kinetics and dissolution mechanisms of albite. *Amer. J. Sci.* **285**, 963-993.

Cornell R. M. and Giovanoli R. (1993) Acid dissolution of hematites of different morphologies. *Clay Minerals* **28**, 223-232.

Cornell R. M., Posner A. M., and Quirk J. P. (1974) Crystal morphology and the dissolution of goethite. *J.Inorg. Nucl. Chem.* **36**, 1937-1946.

Eggleston C. M., Hochella M. F., Jr., and Parks G. A. (1989) Sample preparation and aging effects on the dissolution rate and surface composition of diopside. *Geochim. Cosmochim. Acta* **53**, 797-804.

Fleming B. A. (1986) Kinetics of reaction between silicic acid and amorphous silica surfaces in NaCl solutions. *J. Colloid Interface Sci.* **110**, 40-64.

Fuerstenau D. W. (1970) Interfacial processes in mineral/water systems. *Pure Appl. Chem.* **24**, 135-164.

Furrer G. and Stumm W. (1986) The coordination chemistry of weathering: I. Dissolution kinetics of δ−Al₂O₃ and BeO. *Geochim. Cosmochim. Acta* **50**, 1847-1860.

Gratz A. J. and Bird P. (1993) Quartz dissolution: Theory of rough and smooth surfaces. *Geochim. Cosmochim. Acta* **57**, 977-989.

Hachiya K., Sasaki M., Ikeda T., Mikami N., and Yasunaga T. (1984a) Static and kinetic studies of adsorption-desorption of metal ions on a γ-Al₂O₃ surface. 2. Kinetic study by means of pressure-jump technique. *J. Phys. Chem.* **88**, 27-31.

Hachiya K., Sasaki M., Saruta Y., Mikami N., and Yasunaga T. (1984b) Static and kinetic studies of adsorption-desorption of metal ions on a γ-Al₂O₃ surface. 1. Static study of adsorption-desorption. *J. Phys. Chem.* **88**, 23-27.

Helgeson H. C., Murphy W. M., and Aagaard P. (1984) Thermodynamic and kinetic constraints on reaction rates among minerals and aqueous solutions. II. Rate constants, effective surface area, and the hydrolysis of feldspar. *Geochim. Cosmochim. Acta* **48**, 2405-2432.

Hellmann R. (1995) The albite-water system: Part II. The time-evolution of the stoichiometry of dissolution as a function of pH at 100, 200, and 300 °C. *Geochim. Cosmochim. Acta* **59**, 1669-1697.

Hemingway B. S. (1990) Thermodynamic properties for bunsenite, NiO, magnetite, Fe₃O₄, and hematite, Fe₂O₃, with comments on selected oxygen buffer reactions. *Amer. Mineral.* **75**, 781-790.

Hochella M. F., Jr. and White A. F. (1990) *Mineral-Water Interface Geochemistry, Reviews in Mineralogy*, Vol. 23 (ed. P. H. Ribbe). Mineralogical Society of America, Washington, D.C.

Holdren G. R., Jr. and Berner R. A. (1979) Mechanism of feldspar weathering-I. Experimental studies. *Geochim. Cosmochim. Acta* **43**, 1161-1171.

Holt P. F. and King D. T. (1955) The chemistry of silica surfaces. *J. Chem. Soc. London,* 773-779.

James R. O. and Healy T. W. (1972) Adsorption of hydrolyzable metal ions at the oxide-water interface: I, II and III. *J. Colloid Interface Sci.* **40**, 42-81.

Knauss K. G., Nguyen S. N., and Weed H. C. (1993) Diopside dissolution kinetics as a function of pH, CO₂, temperature, and time. *Geochim. Cosmochim. Acta* **57**, 285-294.

Knauss K. G. and Wolery T. J. (1988) The dissolution kinetics of quartz as a function of pH and time at 70°C. *Geochim. Cosmochim. Acta* **52**, 43-53.

Kraemer S. M. and Hering J. G. (1997) Influence of solution saturation state on the kinetics of ligand-controlled dissolution of oxide phases. *Geochim. Cosmochim. Acta* **61**, 2855-2866.

Lasaga A. C. and Blum A. E. (1986) Surface chemistry, etch pits and mineral-water reactions. *Geochim. Cosmochim. Acta* **50**, 2363-2379.

Malmström M. and Banwart S. (1997) Biotite dissolution at 25°C: The pH dependence of dissolution rate and stoichoimetry. *Geochim. Cosmochim. Acta* **61**, 2779-2799.

Margerum D. W., Cayley G. R., Weatherburn D. C., and Pagenkopf G. K. (1978) Kinetics and mechanisms of complex formation and ligand exchange. In *Coordination Chemistry, Vol. 2*, ACS Monograph 174 (ed. A. E. Martell). American Chemical Society, Washington, D.C. pp. 1-220.

Mast M. A. and Drever J. I. (1987) The effect of oxalate on the dissolution rates of oligoclase and tremolite. *Geochim. Cosmochim. Acta* **51**, 2559-2568.

Maurice P. A., Hochella M. F. Jr., Parks G. A., Sposito G., and Schwertmann U. (1995) Evolution of hematite surface microtopography upon dissolution by simple organic acids. *Clays Clay Mineral.* **43**, 29-38.

Parks G. A. (1965) The isoelectric points of solid oxides, solid hydroxides, and aqueous hydroxo complex systems. *Chem. Rev.* **65**, 177-198.

Parks G. A. (1990) Surface energy and adsorption at mineral-water interfaces: An introduction. In *Mineral-Water Interface Geochemistry* (eds. M. F. Hochella Jr. and A. F. White). Reviews in Mineralogy Vol. 23, Mineralogical Society of America, Washington, D.C. pp. 133-175.

Parks G. A. and de Bruyn P. L. (1962) The zero point of charge of oxides. *J. Phys. Chem.* **66**, 967-973.

Sahai N. and Sverjensky D. A. (1997) Evaluation of internally consistent parameters for the triple-layer model by the systematic analysis of oxide surface titration data. *Geochim. Cosmochim. Acta* **61**, 2801-2826.

Samson S. D. and Eggleston C. M. (1998) Active sites and the non-steady-state dissolution of hematite. *Environ. Sci. Technol.* **32**, 2871-2875.

Samson S. D. and Eggleston C. M. (2000) The depletion and regeneration of dissolution-active sites at the mineral-water interface: II. Regeneration of active sites on α-Fe_2O_3 at pH 3 and pH 6. *Geochim. Cosmochim. Acta* **64**, 3675-3683.

Samson S. D., Stillings L. L., and Eggleston C. M. (2000) The depletion and regeneration of dissolution-active sites at the mineral-water interface: I. Fe, Al, and In sesquioxides. *Geochim. Cosmochim. Acta* **64**, 3471-3484.

Schott J., Berner R. A., and Sjöberg E. L. (1981) Mechanism of pyroxene and amphibole weathering-I. Experimental studies of iron-free minerals. *Geochim. Cosmochim. Acta* **45**, 2123-2135.

Schwertmann U. and Cornell R. M. (1991) *Iron Oxides in the Laboratory: Preparation and Characterization.* VCH Publishers, Inc., New York.

Sjöberg L. (1989) Kinetics and non-stoichiometry of labradorite dissolution. In *Water-Rock Interaction WRI-6* (ed. D. L. Miles). A.A. Balkema, Rotterdam. pp. 639-642.

Spokes L. J. and Jickells T. D. (1996) Factors controlling the solubility of aerosol trace metals in the atmosphere and on mixing into seawater. *Aquatic Geochem.* **1**, 355-374.

Thornton S. D. and Radke C. J. (1988) Dissolution and condensation kinetics of silica in alkaline solution. *SPE Res. Eng.* **May**, 743-752.

Wagman D. D., Evans W. H., Parker V. B., Schumm R. H., Halow I., Bailey S. M., Churney K. L., and Nuttall R. L. (1982) The NBS tables of chemical thermodynamic properties: Selected values for inorganic and C_1 and C_2 organic substances in SI units. *J. Phys. Chem. Ref. Data* **11**(Supplement No. 2), 1-392.

Westall J. C. (1979) MICROQL II. Calculation of adsorption equilibria in BASIC. Swiss Federal Institute of Technology, EAWAG.

Westrich H. R., Cygan R. T., Casey W. H., Zemitis C., and Arnold G. W. (1993) The dissolution kinetics of mixed-cation orthosilicate minerals. *Amer. J. Sci.* **293**, 869-893.

White A. F. and Brantley S. L. (1995) *Chemical Weathering Rates of Silicate Minerals, Reviews in Mineralogy*, Vol. 31 (ed. P. H. Ribbe). Mineralogical Society of America, Washington, D.C.

Wieland E. and Stumm W. (1992) Dissolution kinetics of kaolinite in acidic aqueous solutions at 25°C. *Geochim. Cosmochim. Acta* **56**, 3339-3357.

Wieland E., Wehrli B., and Stumm W. (1988) The coordination chemistry of weathering: III. A generalization on the dissolution rates of minerals. *Geochim. Cosmochim. Acta* **52**, 1969-1981.

Zinder B., Furrer G., and Stumm W. (1986) The coordination chemistry of weathering: II. dissolution of Fe(III) oxides. *Geochim. Cosmochim. Acta* **50**, 1861-1869.